Original Article

Stem hydraulic capacitance decreases with drought stress: implications for modelling tree hydraulics in the Mediterranean oak *Quercus ilex*

Roberto L Salomón[1,2] (iD), Jean-Marc Limousin[3], Jean-Marc Ourcival[3], Jesús Rodríguez-Calcerrada[1] & Kathy Steppe[2]

[1]*Forest Genetics and Ecophysiology Research Group, E.T.S. Forestry Engineering, Technical University of Madrid, Ciudad Universitaria s/n28040 Madrid, Spain,* [2]*Laboratory of Plant Ecology, Department of Applied Ecology and Environmental Biology, Faculty of Bioscience Engineering, Ghent University, Coupure links 653-9000 Ghent, Belgium and* [3]*Centre d'Ecologie Fonctionnelle et Evolutive CEFE, CNRS, UMR 5175, 1919 route de Mende, F-34293 Montpellier, Cedex 5, France*

ABSTRACT

Hydraulic modelling is a primary tool to predict plant performance in future drier scenarios. However, as most tree models are validated under non-stress conditions, they may fail when water becomes limiting. To simulate tree hydraulic functioning under moist and dry conditions, the current version of a water flow and storage mechanistic model was further developed by implementing equations that describe variation in xylem hydraulic resistance (R_X) and stem hydraulic capacitance (C_S) with predawn water potential (Ψ_{PD}). The model was applied in a Mediterranean forest experiencing intense summer drought, where six *Quercus ilex* trees were instrumented to monitor stem diameter variations and sap flow, concurrently with measurements of predawn and midday leaf water potential. Best model performance was observed when C_S was allowed to decrease with decreasing Ψ_{PD}. Hydraulic capacitance decreased from 62 to 25 $kg\,m^{-3}\,MPa^{-1}$ across the growing season. In parallel, tree transpiration decreased to a greater extent than the capacitive water release and the contribution of stored water to transpiration increased from 2.0 to 5.1%. Our results demonstrate the importance of stored water and seasonality in C_S for tree hydraulic functioning, and they suggest that C_S should be considered to predict the drought response of trees with models.

Key-words: holm oak; hydraulic function; process-based modelling; radial stem growth; stem water storage.

INTRODUCTION

As soil dries and atmospheric vapour pressure deficit intensifies, xylem conduits are subjected to lower water potential and may eventually cavitate, thus limiting tree water transport. Xylem vulnerability to drought-induced cavitation has been measured in hundreds of species as the main attribute to quantify tree resistance to drought (Choat *et al.* 2012; Sperry & Love 2015). A growing body of evidence points, however, to a

complementary factor involved in drought resistance: the radial water flow in stems to maintain tree hydraulic integrity by buffering changes in xylem water potential and limiting cavitation of xylem conduits (Goldstein *et al.* 1998; Meinzer *et al.* 2003; Steppe & Lemeur 2004; Scholz *et al.* 2007; Steppe *et al.* 2012; McCulloh *et al.* 2014). In this way, plant tolerance to drought does not solely rely on inherent xylem resistance to cavitation, but also on the radial capacitive release of stored water from elastic-living tissues that transiently reduces xylem tension at a given rate of flow and hence cavitation. Accordingly, a trade-off between hydraulic capacitance and structural traits involved in xylem resistance to cavitation has been observed across a wide range of woody species (Meinzer *et al.* 2008, 2009). Nevertheless, the role of hydraulic capacitance in plant hydraulics has been traditionally overshadowed by the study of drought-induced cavitation and the vulnerability of xylem to changes in water potential (Meinzer *et al.* 2009; McCulloh *et al.* 2014; Epila *et al.* 2017).

Hydraulic modelling is a key tool to mechanistically understand how trees cope with severe and intense drought events (Mencuccini *et al.* 2015; Steppe *et al.* 2015a). Mechanistic models developed for well-watered conditions commonly use static parameters to describe constant xylem hydraulic conductance (Steppe *et al.* 2006, 2008a; Verbeeck *et al.* 2007; Zweifel *et al.* 2007; De Schepper & Steppe 2010), whereas variable hydraulic conductance as a function of water potential has been successfully implemented as the soil dries out (Sperry *et al.* 1998; Baert *et al.* 2015; Mencuccini *et al.* 2015). Likewise, static parameters are used to describe hydraulic capacitance (e.g. Sperry *et al.* 1998; Steppe *et al.* 2006; Zweifel *et al.* 2007; Baert *et al.* 2015); however, none of these models consider the variability in stem hydraulic capacitance, although stem water reservoirs are progressively depleted under dry conditions (Scholz *et al.* 2007, 2008; Verbeeck *et al.* 2007; Betsch *et al.* 2011; Kocher *et al.* 2013; Matheny *et al.* 2015). Accounting for the dynamic drought response of both hydraulic conductance and capacitance could improve model performance under a wide range of environmental conditions and extended time frames (Steppe *et al.* 2008b). Model refinement via integration of tree drought responses has therefore been encouraged to advance in our mechanistic understanding of tree hydraulic

Correspondence: R. L. Salomón. E-mail: RobertoLuis.SalomonMoreno @UGent.be

functioning in future drier scenarios (Verbeeck *et al.* 2007; Baert *et al.* 2015; Mencuccini *et al.* 2015; Steppe *et al.* 2015a, 2015b).

In this study, we aimed at modelling tree hydraulic functioning in field-grown *Quercus ilex* L. under wet to dry conditions by taking into account the dynamic nature of both xylem resistance to water transport (R_X) and stem hydraulic capacitance (C_S). For this purpose, process-level equations that describe the relationship of R_X and C_S with predawn water potential (Ψ_{PD}) have been implemented in the current version of a sophisticated mechanistic model that integrates tree water transport dynamics and stem diameter variations (Steppe *et al.* 2006, 2008a; De Swaef *et al.* 2015). Water reservoirs are defined here as the elastic tissues subjected to reversible diel cycles of water release and refill to avoid xylem cavitation. Inelastic water release from cavitated xylem conduits under negative water potential (Tyree & Ewers 1991; Hölttä *et al.* 2009) is neglected because the rapid reversibility of this phenomenon remains a matter of debate (Brodersen & McElrone 2013; Cochard & Delzon 2013). An advantage of this approach is that measurements are not destructive, because the model is driven by sap flow and Ψ_{PD}, and calibrated against stem diameter variations and xylem water potential at midday. As these variables can be monitored with peripheral devices and by sampling a small number of leaves, the hydraulic functioning of surveyed trees can be continuously modelled, and research is not restricted to discrete observations.

We hypothesize that including daily variations in R_X and C_S as a function of Ψ_{PD} improves model accuracy in predicting stem diameter variations and xylem water potential during the dry season. Contrarily, we predict that variability in R_X and C_S may not improve model performance during the wet season as R_X and C_S are expected to remain constant. The integrated root-to-leaf R_X was modelled as function of Ψ_{PD} using a negative exponential curve (Baert *et al.* 2015), an alternative approach to estimate the integrated root-to-leaf hydraulic conductance ($K_X = 1/R_X$) and generate vulnerability curves. Furthermore, a new equation defining the relationship between C_S and Ψ_{PD} was developed using the shape of water desorption curves and cumulative water release curves reported for several species (Zweifel *et al.* 2000; Meinzer *et al.* 2003, 2009; Steppe *et al.* 2006; Barnard *et al.* 2011; McCulloh *et al.* 2014). Both magnitude of the decrease in C_S during the dry season and contribution of stored water to the transpiration stream were evaluated. Simulated cumulative water release from internal storage pools was compared with estimates of stem water refilling at the end of the dry season after first autumn heavy rains. Likewise, the simulated vulnerability curve was compared to the vulnerability curves obtained by measurements at the organ scale in the same experimental site (Limousin *et al.* 2010a; Martin-StPaul *et al.* 2014).

MATERIALS AND METHODS

Site description

The study site is located in the Puéchabon State Forest (Montpellier, France) in a stand dominated by *Q. ilex* (43°44′29″ N, 3°35′45″ E, 270 m.a.s.l.). The stand has been historically subjected to periodic coppicing, with the last cut being performed in 1942. Nowadays, top canopy height is 5.5 m, stand density is 4700 stems ha^{-1} and most stems (>70%) range in diameter at breast height from 4 to 10 cm. *Buxus sempervirens* L., *Phyllirea latifolia* L., *Pistacia terebinthus* L. and *Juniperus oxycedrus* L. are the main species of the understory layer. The area has a Mediterranean-type climate: annual mean temperature is 13.4 °C, annual precipitation is 907 mm and 80% of this amount falls during winter and autumn, when temperatures are lower (Limousin *et al.* 2009). A weather station located at the experimental site was used to monitor meteorological conditions. Air temperature, relative humidity (MP100, Rotronic, Bassersdorf, Switzerland) and rainfall (tipping bucket rain gauge ARG100, Environmental Measurements Ltd, Sunderland, UK) were measured every minute and averaged every 30 min with a data logger (model 21X, Campbell Scientific Ltd, Shepshed, UK). More details on the experimental site are available in Rambal *et al.* (2014).

Tree and soil measurements

Six *Q. ilex* trees (Table 1) were instrumented to continuously monitor sap flow and stem diameter variations. We selected data from the year 2009 because it was characterized by a strong and typical summer drought between mid-July and mid-September, and due to data availability on leaf water potential at predawn and midday in the instrumented trees during the summer.

Sap flux density (g cm^{-2} h^{-1}) was continuously monitored with thermal dissipation probes (Granier 1985). Probe pairs were inserted at 1.2 m height with a vertical separation of 10 cm. Probes were oriented facing north to avoid direct solar heating and were protected from rain and radiation by aluminium cover. Temperature difference between the probes was registered every 5 min, and averaged and recorded every 30 min with a data logger (model CR10X, Campbell Scientific). Sap flux density was calculated considering zero flow from the absolute maximum temperature difference over 2 d running periods. Sap flux density was upscaled to the tree level to obtain sap flow (F_{STEM}, g h^{-1}) by multiplying sap flux density by sapwood area. Sapwood area was estimated from an allometric relationship between tree diameter at breast height and sapwood area obtained from 18 additional trees (Limousin *et al.*

Table 1. Diameter at breast height (DBH), tree height, accumulated diameter increment and mean daily sap flow during 2009 for the six monitored *Quercus ilex* trees

	DBH (cm)	Height (m)	Annual diameter increment (mm year^{-1})	Mean sap flow (kg day^{-1})
TREE1	9.55	5.3	0.25	2.55
TREE2	11.05	5.0	0.16	3.00
TREE3	10.70	5.0	0.51	5.87
TREE4	13.20	5.6	1.21	7.32
TREE5	10.05	5.2	−0.10	2.90
TREE6	12.25	4.5	1.15	3.00

Tree DBH measured at the beginning of the 2009 growing season.

2009). For further details about F_{STEM} measurements, see Limousin *et al.* (2009).

Stem circumference variations were recorded using automatic band dendrometers (ELPA-98, University of Oulu, Oulu, Finland). Dendrometers were just below the thermal dissipation probes, and the outer layer of dead bark was removed prior to installation. Circumference variations were registered every 5 min and recorded every 30 min with a data logger (model CR1000; Campbell Scientific Ltd, Shepshed, UK) and transformed to stem diameter variations (ΔD, μm). For further details about ΔD measurements, see Lempereur *et al.* (2015).

Leaf water potential (Ψ_{LEAF}, MPa) was measured with a pressure chamber (PMS1000, PMS Instruments, Corvallis, OR, USA) on DOYs 114, 176, 208, 234 and 310 during the 2009 growing season (23 April, 24 June, 26 July, 21 August, 5 November, respectively) at predawn (before 06:00 h) and midday (14:00 h). Two leaves were sampled per tree, and a third leaf was sampled if the observed difference between measurements was higher than 0.2 MPa. Samples were taken at similar tree heights, and measurements were performed within 1 min after leaf excision. Leaf water potential was measured in four of the six trees instrumented for F_{STEM} and ΔD measurements. Average Ψ_{LEAF} of these four trees was used for the two remaining trees.

The discrete measurements of Ψ_{PD} were interpolated on a daily basis using modelled soil water storage (SWS, mm). Daily SWS was modelled using the soil water balance module of the SIERRA vegetation model driven by daily values of solar radiation, minimum and maximum temperature and precipitation (Mouillot *et al.* 2001; Ruffault *et al.* 2013). Soil water storage and Ψ_{PD} were related by a Campbell-type retention curve (Campbell 1974). The SWS model was validated against measurements of SWS integrated over a rooting depth of 4.5 m and performed at approximately monthly intervals from 1998 to 2009 using a neutron moisture gauge (see Rambal *et al.* 2003 for further details). The relationship between modelled and measured SWS displayed a good agreement ($R^2 = 0.92$; $P < 0.0001$; RMSE = 16 mm; $n = 90$), as well as the relationship between modelled and measured Ψ_{PD} ($R^2 = 0.73$; $P < 0.0001$; RMSE = 0.71 MPa; $n = 95$). Despite the good fit obtained between SWS and Ψ_{PD} on an annual basis, Ψ_{PD} was underestimated by the soil water balance model during summer drought. To correct daily simulated values of Ψ_{PD} in summer, optimized parameters for each tree were selected to account for spatial heterogeneity in leaf area index, soil texture and stone fraction.

Mechanistic tree modelling

Model description

The current version of a mechanistic water flow and storage model (Steppe *et al.* 2008a) was used to study the hydraulic functioning of *Q. ilex* trees. Briefly, the model is composed of two interconnected sub-models describing dynamics in tree water transport and stem diameter variations, in which F_{STEM} dynamics are intimately linked to stem ΔD by radial water flow between the xylem and the outer tissues. Note that 'stem' refers

to the tree trunk, so that branches are excluded for model simplicity. The model assumes the xylem as a rigid cylinder (xylem compartment) surrounded by an elastic outer ring composed of cells of cambium, phloem and bark (storage compartment) responsible for diel shrinkage and swelling (Steppe *et al.* 2006). Therefore, the water stored in outer elastic cells constitutes the only capacitive water source; water release from the xylem parenchyma and cavitated conduits is neglected by this model. Sap flow (F_{STEM}) integrates the axial water flow through the xylem compartment via root water uptake (f_X) and the radial water exchange between xylem and storage compartment (f_S). Axial water flow (f_X) is calculated as the water potential gradient between the roots and the stem divided by R_X, and radial water flow (f_S) is calculated as the first derivative defining the change in water content of the storage compartment, which is influenced by the resistance to radial flow between xylem and storage compartment (R_S, MPa h g^{-1}). The model equations are shown in the Supporting Information (Note S1). When transpiration starts, a water potential gradient between xylem and storage compartment ($\Psi_X - \Psi_S$) leads to radial flow from outer cells to the xylem to fulfil the transpiration need; Ψ_X is inferred from Ψ_{LEAF} measurements (see below), whereas Ψ_S is estimated as a function of the water content and capacitance of the storage compartment (see Note S1). Water depletion in the morning results in reduction in cell turgor and reversible stem shrinkage. Conversely, water refilling in the afternoon, when atmospheric vapour pressure deficit and transpiration start to decline, results in reversible stem swelling. Water potential in the storage compartment is the algebraic sum of the osmotic potential (Ψ_S^O) and the turgor pressure (Ψ_S^P). Irreversible stem growth occurs when carbon requirements are met (Daudet *et al.* 2005) and turgor pressure exceeds a threshold value for cell wall yielding (Γ, Lockhart 1965). For a detailed explanation of the principles of the model, see Steppe *et al.* (2006, 2008a) and De Pauw *et al.* (2008).

To allow variation in xylem hydraulic resistance of the root-to-leaf continuum (R_X, MPa h g^{-1}) and stem hydraulic capacitance (C_S, g MPa^{-1}), the model was further developed by implementing two equations and their corresponding parameters:

The hydraulic resistance was described to vary exponentially with Ψ_{PD} (Baert *et al.* 2015), which accounted for day to day variations in R_X with soil drying while assuming no daily refilling of cavitated xylem:

$$R_X = r_1 \, e^{\left(\Psi_{PD}^2 \right) r_2} \tag{1}$$

where r_1 (MPa h g^{-1}) and r_2 (MPa^{-2}) are the proportionality parameters influenced by plant characteristics.

The hydraulic capacitance of the stem was calculated as the derivative of the water release curve (Steppe *et al.* 2006):

$$C_S = \frac{dW}{d\Psi} \tag{2}$$

where dW is the variation in water content in the storage compartment (g h^{-1}) and $d\Psi$ the corresponding variation in Ψ (MPa h^{-1}). In this study, the cumulative water (W) release curve was defined by a logarithmic equation of similar shape

to those previously reported (e.g. Meinzer *et al.* 2003, 2009; McCulloh *et al.* 2014):

$$W = - log_{w_1}(w_2 \Psi + 1) \tag{3}$$

where w_1 and w_2 are the parameters defining the shape of the water release curve. The derived form of Eqn 3 results in an inverse equation between C_S and Ψ_{PD}:

$$C_S = \frac{1}{(c_1 \Psi_{PD} + c_2)} \tag{4}$$

where c_1 (g^{-1}) and c_2 (MPa g^{-1}) are the proportionality parameters dependent on plant properties, which are related to the parameters defining the water release curve (Eqn 3) as follows: $w_1 = e^{c_1}$, and $w_2 = \frac{ln(w_1)}{c_2}$. Note that the purpose of this study is to evaluate seasonality in R_X and C_S. Therefore, R_X and C_S in this model fluctuate on a daily basis with Ψ_{PD}, so that both are assumed constant within 24 h periods as diel variability in R_X and C_S is expected to be comparatively negligible (see Baert *et al.* 2015).

Four models were calibrated for each tree: (1) R_X and C_S were assumed to be constant (the simplest framework, used for model calibration of R_X and C_S); (2) R_X was allowed to vary, and C_S was assumed to be constant (model calibration of r_1, r_2 and C_S); (3) C_S was allowed to vary, and R_X was assumed to be constant (model calibration of R_X, c_1 and c_2); and (4) both R_X and C_S were allowed to vary (model calibration of r_1, r_2, c_1 and c_2). The resistance to radial flow between xylem and storage compartment (R_S) was also calibrated in each model.

Model simulation, calibration and identifiability analyses

Model simulations, calibrations and identifiability analyses were performed using the plant modelling software PhytoSim (version 2.1, Phyto-IT, Mariakerke, Belgium). Simulations were conducted with a fourth-order variable step size solver of an accuracy of 10^{-6} and a maximum step size of 1 h. Calibrations were done using the simplex method to minimize the weighted sum of squared errors (SSE) for ΔD and Ψ_X. Identifiability analyses were performed to check whether the subset of model parameters to calibrate was not correlated and sensitive enough and thus was identifiable (De Pauw *et al.* 2008). A collinearity index (CI) above 15 indicated an unidentifiable subset of parameters. Values of non-calibrated model parameters were directly measured or assigned from literature (Table S1 in Supporting Information).

Predawn water potential and F_{STEM} were used as model inputs, and ΔD and Ψ_X were used for calibration purposes. The best model was selected using the final predicted error (FPE) criteria (Steppe *et al.* 2006):

$$FPE = \frac{SSE}{N} + \frac{2pSSE}{(N-p)N} \tag{5}$$

where SSE is the weighted sum of squared errors for ΔD and Ψ_X, N is the number of observations and p the number of calibrated parameters. The first term of the FPE evaluates the goodness of fit between measured and simulated data, whereas the second term penalizes over-parameterized models. Thus, the smaller the FPE value, the better the model.

Because rain events and tree trembling resulted in irregular signals recorded by the automatic band dendrometers, data were manually inspected to select a set of days that displayed reliable diel patterns, that is, smooth morning shrinkage and afternoon swelling. As the number of ΔD observations after manual inspection differed among trees, FPE values also differed. To remove any effect associated to the number of observations, values of FPE were normalized relative to the simplest framework (constant R_X and C_S) for each tree.

Models were calibrated under wet and dry conditions. As stem growth during the summer season is limited by soil water availability in the surveyed site (Lempereur *et al.* 2015), wet and dry periods were defined according to growing or non-growing conditions, respectively. Periods that cover two consecutive midday Ψ_{LEAF} measurements were initially considered for model calibration: DOYs 113–177 were selected for the wet period (spring and early summer) and DOYs 207–235 for the dry period (late summer). Inaccurate simulations were initially obtained during the wet period, and further attempts to improve simulations were tested. First, the stem growth curve was adjusted to a Gompertz-shaped curve (Winsor 1932) to smooth large fluctuations registered by the band dendrometers (Fig. 1d); and second, a shorter time period around a single Ψ_{LEAF} measurement campaign (DOY 176, early summer) was additionally examined.

To calibrate the models, midday Ψ_X was inferred from midday Ψ_{LEAF} measurements. Under dry conditions, measurements of midday Ψ_{LEAF} could be used as a surrogate of midday Ψ_X, because of the strong stomatal limitation observed in the monitored trees (see Fig. 3 in Limousin *et al.* 2010b), which minimized the disequilibrium in water potential between xylem and leaves (Meinzer *et al.* 2009). In contrast, substantial disequilibrium between midday Ψ_{LEAF} and midday Ψ_X might occur when water is not limiting, as has been observed in *Q. ilex* seedlings (Rodríguez-Calcerrada *et al.* 2017) and in Neotropical savanna trees (see Fig. 2 in Scholz *et al.* 2007). Under wet conditions, the difference between midday and predawn Ψ_X ($\Delta\Psi_X$ = midday Ψ_X − predawn Ψ_X) was assumed as a constant fraction of $\Delta\Psi_{LEAF}$ ($\Delta\Psi_{LEAF}$ = midday Ψ_{LEAF} − predawn Ψ_{LEAF}). The ratio $\Delta\Psi_X / \Delta\Psi_{LEAF}$ was obtained from measurements performed in *Q. ilex* seedlings ($\Delta\Psi_X / \Delta\Psi_{LEAF}$ = 0.342; Fig. S1 in Supporting Information), in which leaves were covered with aluminium foil for 1 h to measure Ψ_X. Midday Ψ_X was therefore estimated as a function of Ψ_{PD} and $\Delta\Psi_{LEAF}$ (midday $\Psi_X = \Psi_{PD} + 0.342 \times \Delta\Psi_{LEAF}$). By using this approximation of Ψ_X, we made the assumptions that leaf hydraulic resistance was a constant fraction of the tree hydraulic resistance independently of tree size (Sack *et al.* 2003), that the water potential difference between leaves and stem depended mainly on leaf transpiration and that the Ψ_X difference between the trunk and the branches was negligible.

Stem water refilling measurements

Stem water refilling was estimated by integrating sap flow over intense rain events at the end of summer drought. We only
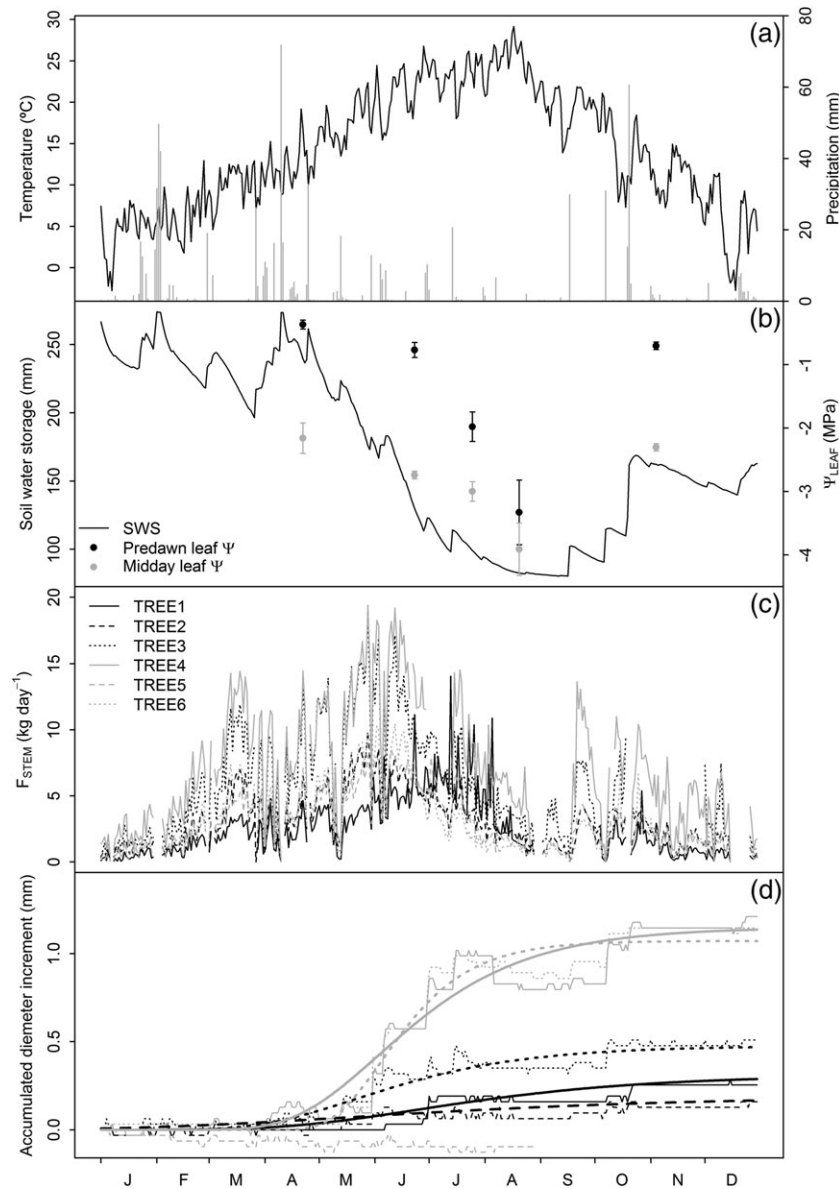
Figure 1. Daily air temperature and precipitation (a), soil water storage and predawn and midday leaf water potential (means ± SE; b), daily sap flow (c) and daily stem diameter variations (d) during the year 2009. Ecophysiological measurements were performed on six *Quercus ilex* trees of the experimental site. Curves of accumulated diameter increment were smoothed according to the Gompertz's equation (dashed lines). Diel variations in diameter are not shown for clarity.

considered short (<4 h) and heavy (>20 mm) rainfall events occurring at night or in the late evening to ensure that recorded sap flow could be attributed to stem water refilling and not to leaf transpiration (Betsch *et al.* 2011), and to avoid rainfall events that resulted in slow refilling extending beyond night-time. Sap flow was integrated along the rain event and following night-time hours to estimate the volume of water refilled. Stem water refilling was then divided by the corresponding shift in Ψ_{PD} measured before and after the rain event to estimate C_S (Eqn 2) and compare it with values obtained from model simulations. Available measurements of Ψ_{PD} obtained less than one week before and after the rainfall event were necessary to calculate C_S. As the first heavy rain in 2009 did not meet these requirements, different years were inspected, and

suitable rain events were found in 2006 and 2007 to estimate C_S. TREE4 was excluded from this analysis, as it was not monitored in 2006 and 2007. However, 18 *Q. ilex* trees located in the study site and equipped with thermal dissipation probes were additionally included.

Data analyses

To compare model performance (i.e. normalized FPE) among the four tested models and the two surveyed periods, Tukey's multiple comparison tests were performed using the *TukeyHSD* function in the R software (version 3.2.3). The best model was then selected to obtain R_X and C_S along the gradient of Ψ_{PD} on a per-tree basis. To test whether F_{STEM} and

radial water flow (f_S) varied with Ψ_{PD}, mixed models were adjusted using the *lme* function in the nlme library, in which stem was considered as a random factor ($n = 6$). As the model output for C_S refers to the whole tree, C_S was standardized per unit of storage volume. The storage volume was estimated as the product of stem height by stem basal area subtracting the xylem compartment. The integrated root-to-leaf hydraulic conductance was calculated as the inverse of the integrated root-to-leaf hydraulic resistance ($K_X = 1/R_X$, g MPa^{-1} h^{-1}). Predawn water potential causing 50% loss of K_X (Ψ_{50}) was obtained following Baert *et al.* (2015). To obtain the mean curve and confidence intervals of C_S, cumulative water release and integrated root-to-leaf R_X and K_X along the gradient of Ψ_{PD}, uncertainty analyses were performed in PhytoSim using the averaged parameters among the six studied trees yielded by the best model. All values presented in the text are means ± SE.

RESULTS

Averaged among the six surveyed stems and across the whole year, daily sap flow was 4.11 ± 0.81 kg day^{-1} (Fig. 1c, Table 1), and mean annual diameter increment was 0.53 ± 0.20 mm year^{-1} (Fig. 1d, Table 1). During spring and early summer (DOYs 113–177), average temperature was 18.2 °C and accumulated rainfall 107.2 mm. Late summer was hot and dry, with an average temperature of 25.2 °C and an accumulated rainfall of 11.8 mm during the dry modelled period (DOYs 207–235). The lowest Ψ_{LEAF} was measured at the end of this period, when it reached mean values of -3.3 MPa at predawn and -3.9 MPa at midday (Fig. 1b).

Four models with constant or variable R_X and C_S were adjusted per tree and period to simulate ΔD and Ψ_X over time. A consistent pattern was observed under wet (Fig. 2a) and dry (Fig. 2b) conditions. Relative to the simplest model (constant R_X and C_S), the normalized FPE was not reduced when R_X alone was allowed to vary ($P > 0.1$). In contrast, the normalized FPE was reduced ($P < 0.001$) when C_S was allowed to vary with Ψ_{PD}. The model with variable R_X and C_S showed the lowest normalized FPE, although its value did not differ significantly from that obtained with constant R_X and variable C_S ($P > 0.1$). Therefore, calibration of the model with a variable C_S was the main improvement required to accurately simulate ΔD and Ψ_X. Only data yielded by the best model (variable R_X and C_S) are shown hereafter.

Models were calibrated under wet and dry conditions. Only TREE5 was not modelled during the wet season due to the inconsistent dendrometer signal at the time of Ψ_{LEAF} measurement. Because of concurrent stem growth, inaccurate simulations of ΔD were initially obtained during the wet period when considering long temporal spans (DOYs 113–177; data not shown). Shorter temporal spans of 3–4 d resulted in realistic simulations of Ψ_X and ΔD (Fig. 3a–c, FPE = 6.04 ± 1.90). The length of the simulation period was not an issue under dry conditions when stem growth was impeded, and accurate simulations were obtained for every tree throughout the 1 month simulated period (Fig. 3d–f, FPE = 7.71 ± 2.11). During the wet season, cell turgor pressure at night-time was higher than the turgor threshold for cell wall yielding ($\Psi_S^P > \Gamma$, Fig. 3a)
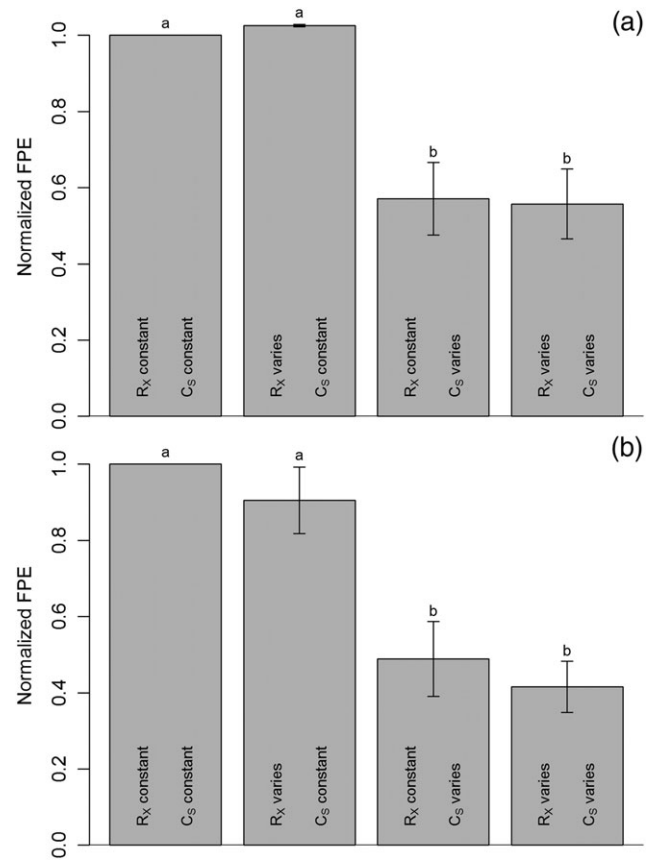

Figure 2. Normalized final prediction error (FPE) of four tested models with constant or variable hydraulic resistance (R_X) and capacitance (C_S) to compare model performance. Models were used to simulate hydraulic functioning of *Quercus ilex* trees under wet (a) and dry (b) conditions. The FPE evaluates the accuracy of simulated diameter variations (ΔD) and xylem water potential (Ψ_X) and penalizes over-parameterized models. Low FPE values indicate better model performance. Values of FPE were normalized relative to the model with constant R_X and C_S to remove inter-stem variability associated to the number of observations. Normalized FPE was averaged among six trees. Different letters show significant differences ($P < 0.05$).

leading to irreversible stem growth (Fig. 3b). During the dry season, soil drying progressively reduced Ψ_X, Ψ_S and cell osmotic potential, which explained the rather constant pattern of cell turgor pressure, which was below the turgor threshold for cell wall yielding ($\Psi_S^P < \Gamma$, Fig. 3d), thus impeding irreversible stem growth (Fig. 3e). Morning stem shrinkage and afternoon stem swelling (Fig. 3b,e) were caused by the radial water flow between xylem and storage compartments (f_S, Fig. 3c,f).

Daily F_{STEM} was directly related to Ψ_{PD} in every surveyed stem ($P < 0.01$, Fig. 4a). Averaged among the six stems, F_{STEM} decreased from 7.50 ± 0.83 kg day^{-1} during the wet period ($\Psi_{PD} = -1.0$ MPa) to 1.46 ± 0.81 kg day^{-1} at the end of the dry period ($\Psi_{PD} = -3.3$ MPa, $P < 0.001$). The decrease in daily stem water release from the storage to the xylem compartment (daily sum of negative f_S, hereafter daily $|f_S|$, in kg day^{-1}) with Ψ_{PD} was significant in only half of the surveyed trees ($P < 0.05$, Fig. 4b) and became non-significant when pooling trees across
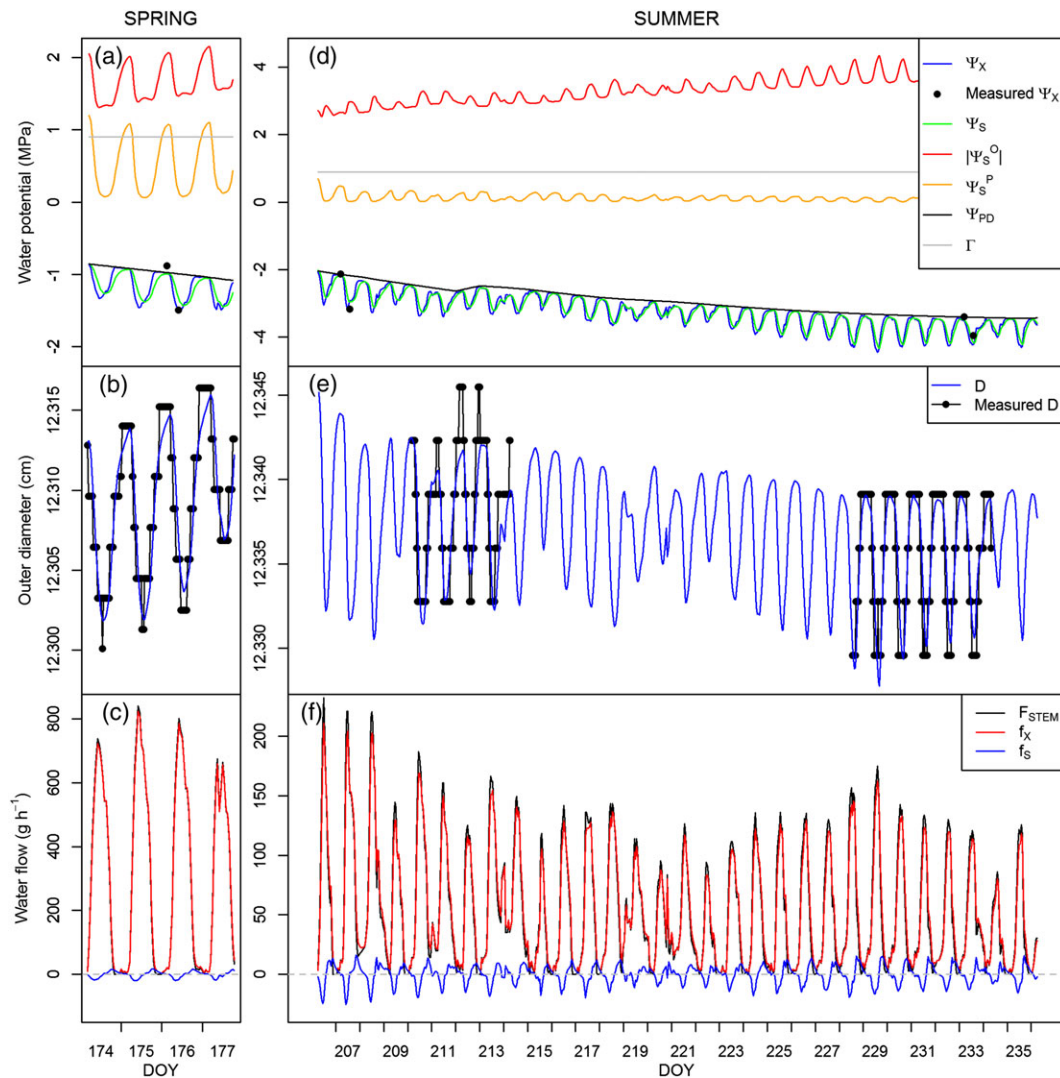
Figure 3. Measured and simulated water potentials (a, d), diameter variations (b, e) and water flows (c, f) in *Quercus ilex* trees during the wet (a–c) and the dry (d–f) season. Predawn water potential (Ψ_{PD}) and sap flow (F_{STEM}) (continuous black lines) were used as model inputs, whereas diameter variations and xylem water potential (Ψ_X) (black dots) were used for calibration purposes. This figure displays an example of model simulation for a single tree (TREE6) when the hydraulic resistance and hydraulic capacitance were allowed to vary with predawn water potential (best model obtained). Under well-watered conditions, cell turgor (Ψ_S^P) at night-time exceeded the critical value for wall-yielding (Γ) (a) resulting in irreversible stem growth (b). During summer drought, Ψ_S^P never exceeded Γ (d) and irreversible stem growth was impeded (e). The storage compartment supplied water to the xylem to fulfil transpiration requirements during the morning (negative f_S) and was refilled during the afternoon (positive f_S) (c, f). Radial water exchange caused diel patterns of stem shrinkage and swelling. Note different scales for the same variables in wet and dry periods. Note that absolute values of osmotic water potential (Ψ_S^O) are displayed for clarity.

a range of Ψ_{PD} from -1.0 to -3.3 MPa ($P = 0.15$). Considering the dry period only, daily $|f_S|$ significantly decreased with Ψ_{PD} ($P < 0.001$) from 0.13 ± 0.03 to 0.10 ± 0.03 kg day^{-1} for a corresponding reduction in Ψ_{PD} of 1.3 MPa (from -2.0 to -3.3 MPa). Across the year, daily sap flow was reduced to a greater extent than daily $|f_S|$ as the soil dried out. Hence, the daily contribution of $|f_S|$ to F_{STEM} increased with drought severity ($P < 0.001$) from $2.0 \pm 0.9\%$ to $5.1 \pm 0.9\%$ when Ψ_{PD} decreased from -1.0 to -3.3 MPa (Fig. 4c).

Stem hydraulic capacitance decreased with drought stress. Mean C_S on a storage volume basis was 61.69 ± 6.30 kg MPa^{-1} m^{-3} under wet conditions (Table 2) and reached lowest values of 24.93 ± 4.14 kg MPa^{-1} m^{-3} at

the end of the summer drought (Table 3). Figure 5a illustrates the mean cumulative release of water from storage compartments and the change in C_S at the tree level obtained in the dry period and extrapolated to a wider range of Ψ_{PD}. Hydraulic capacitance obtained from model calibration during the wet period ($C_S = 314.51 \pm 38.83$ g MPa^{-1} tree^{-1}) was underestimated by the C_S curve extrapolated from the dry period. Similarly, Fig. 5b displays mean R_X and K_X curves obtained in the dry period. The vulnerability curve of root-to-leaf hydraulic conductance obtained from the dry period showed a mean Ψ_{50} value of -2.67 ± 0.23 MPa (Table 3). The R_X value obtained from direct model calibration under wet conditions ($5.01 \pm 0.45 \times 10^{-4}$ MPa h g^{-1}, Table 2) was
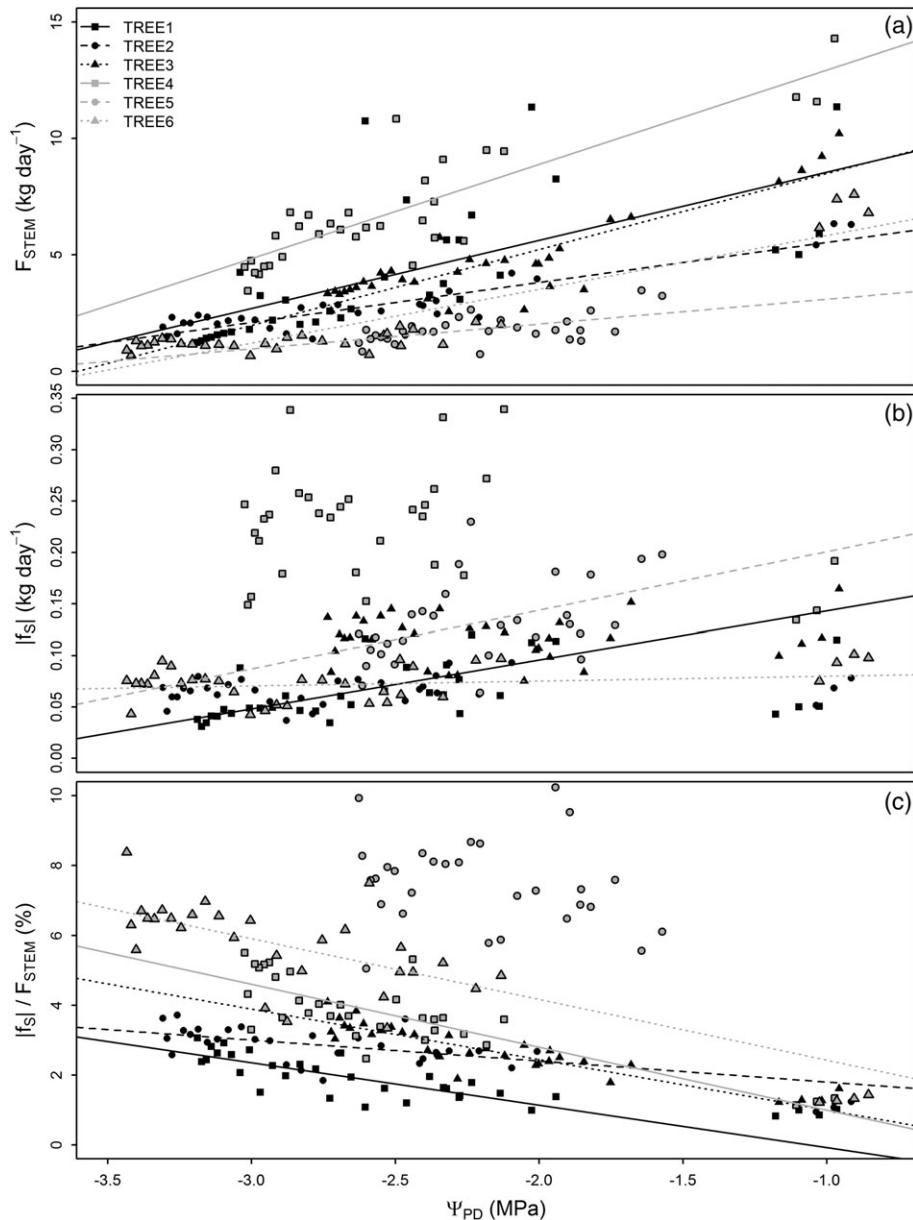
Figure 4. Variation in daily sap flow (a; F_{STEM}), daily stem water release (b; $|f_S|$), and the contribution of $|f_S|$ to F_{STEM} (c) in *Quercus ilex* trees along a gradient of predawn water potential (Ψ_{PD}). Data from model simulations in early summer (wet period) and summer drought (dry period) are pooled. Only significant regressions are depicted ($P < 0.05$).

overestimated by the R_X curve extrapolated from summer drought.

Two rain events were used to independently estimate C_S from stem water refilling. In 2006, 24 mm of rainfall was registered during the night of DOY 228 to 229, whereas in 2007, a stronger rainfall of 75.5 mm occurred in the night of DOY 261 to 262. The corresponding mean increase in Ψ_{PD} was 2.6 and 2.9 MPa for 2006 and 2007, respectively. Stem water refilling and C_S on a tree basis were exponentially related to stem size across the 23 trees examined ($P < 0.001$; Fig. 6). Average stem water refilling and C_S among the five trees monitored in both approaches were 1134 ± 149 g tree^{-1} and 414 ± 45 g MPa^{-1} tree^{-1}, respectively.

DISCUSSION

The importance of a variable hydraulic capacitance in tree modelling

Hydraulic capacitance is commonly measured as the slope of the initial and nearly linear portion of the curve between the cumulative water release and water potential (Meinzer *et al.* 2003, 2008; Barnard *et al.* 2011; McCulloh *et al.* 2014). These estimates of C_S are therefore obtained within the range of Ψ_X when plants are not subjected to drought stress. Notwithstanding, C_S varies seasonally as water storage refilling is limited by soil drying (Verbeeck *et al.* 2007; Scholz *et al.* 2008; Steppe *et al.* 2008b; Kocher *et al.* 2013; Matheny *et al.* 2015). Progressive

Table 2. Hydraulic resistance to radial flow between the xylem and the storage compartment (R_S), hydraulic resistance of the root-to-leaf segment (R_X) and stem hydraulic capacitance (C_S) obtained from the mechanistic water flow and storage model describing the hydraulic functioning of *Quercus ilex* trees during the wet season when stem growth occurred

	R_s	R_X	C_S
	(MPa h g^{-1}) 10^{-2}	(MPa h g^{-1}) 10^{-4}	(kg MPa^{-1} m^{-3})
TREE1	0.97	4.59 [4.59–4.59]	64.02 [54.66–72.22]
TREE2	1.41	5.72 [5.72–5.72]	50.06 [45.03–54.79]
TREE3	0.93	4.59 [4.59–4.59]	86.07 [73.33–98.28]
TREE4	0.53	3.65 [3.62–3.69]	61.38 [54.98–66.94]
TREE5[a]	NA	NA	NA
TREE6	1.15	6.49 [6.38–6.62]	46.91 [41.67–52.69]
mean (SE)	1.00	5.01	61.69
	(0.13)	(0.45)	(6.30)

R_S was assumed constant whereas R_X and C_S were allowed to vary with predawn water potential (Eqns 1 and 4, respectively). The modelled period lasted 3–4 d and included DOY176, when leaf water potential was measured. Mean values of R_X and C_S on a storage volume basis are shown; minimum and maximum values for this period are indicated in square brackets.
[a]TREE5 was not modelled due to an inconsistent dendrometer signal.

decoupling between daily capacitive water discharge and daily water refilling leads to water reserves depletion, and accordingly, a net reduction in stem diameter is commonly observed during the dry season (Fig. 3e; Zweifel *et al.* 2000; Lempereur *et al.* 2015). Progressive depletion of water reservoirs should be incorporated in process-based hydraulic models by the implementation of a direct relationship between C_S and soil water availability. However, to the best of our knowledge, no mechanistic model has yet considered drought-induced variability in C_S to model tree hydraulic functioning. Furthermore, and unexpectedly, considering the variation of C_S with Ψ_{PD} was also found to result in more accurate simulations of Ψ_X and ΔD during the wet period. In contrast to previous studies using this

model in which C_S was assumed constant under well-watered regimes and stable soil water content (e.g. Steppe *et al.* 2006, 2008a; De Schepper & Steppe 2010), considering a variable C_S was here necessary to simulate the increase in turgor that yielded irreversible cell wall extension. Assuming a constant C_S in our study resulted in a progressive reduction of maximum daily turgor pressure that impeded stem growth (simulations not shown) as Ψ_{PD} slightly declined during this 'wet' period (Fig. 3a). Consequently, under both wet and dry conditions, assumptions of constant C_S may partially explain why tree models fail to reproduce variations in diameter and Ψ_X in environments where soil water availability fluctuates. We suggest that to better predict and understand tree hydraulic functioning and the risk of hydraulic failure in dry regions, it is necessary to take into account the dynamic nature of C_S.

Because C_S is commonly measured under moist conditions, estimates of C_S on a storage volume basis in early summer (62 kg m^{-3} MPa^{-1}, Table 2) might be more appropriate for literature comparison. Hydraulic capacitance of *Q. ilex* at this time of year was consistent with the reported range for evergreen sclerophyll species (6–102 kg m^{-3} MPa^{-1}, Richards *et al.* 2014) and lower than the ones for tropical species (70–420 kg m^{-3} MPa^{-1}, Meinzer *et al.* 2003, 2009) and conifers (107–886 kg m^{-3} MPa^{-1}, Barnard *et al.* 2011; McCulloh *et al.* 2014). Nevertheless, neglecting the xylem tissues as capacitive water sources might lead to underestimation of the overall hydraulic capacitance of *Q. ilex* stems in our study. Hydraulic capacitance decreased across the season from 62 to 25 kg m^{-3} MPa^{-1} (from DOY 176 to 235, respectively). The 60% reduction in C_S illustrates the importance of implementing variable C_S in mechanistic models to accurately simulate tree water status and diameter variations. Our modelling approach further allowed estimation of the daily contribution of internal water storage to total daily sap flow ($|f_S| / F_{STEM}$) as a function of Ψ_{PD}. The average $|f_S| / F_{STEM}$ ratio ranged between 2% in early summer and 5% at the end of summer drought when Ψ_{PD} reached mean values of −3.3 MPa (Fig. 4c). This ratio is

Table 3. Calibrated parameters used in the mechanistic water flow and storage model describing the hydraulic functioning of *Quercus ilex* trees during summer drought when stem growth was impeded. The hydraulic resistance (R_X) and hydraulic capacitance (C_S) were allowed to vary with predawn water potential (Ψ_{PD}). Estimates of C_S and the Ψ_{50} from the vulnerability curve were obtained from model simulations

	Calibrated parameters[a]					C_S[b]		Ψ_{50}[c]
	R_s	c_1	c_2	r_1	r_2	DOY208	DOY234	
	(MPa h g^{-1}) 10^{-2}	(g^{-1}) 10^{-3}	(MPa g^{-1}) 10^{-3}	(MPa h g^{-1}) 10^{-3}	(MPa^{-2}) 10^{-1}	(kg MPa^{-1} m^{-3})		(MPa)
TREE1	1.95	−3.07	2.68	0.99	1.29	26.52	18.48	−2.32
TREE2	1.73	−2.54	2.01	1.68	0.67	28.91	19.84	−3.21
TREE3	2.30	−2.33	2.78	1.26	1.53	31.75	23.34	−2.13
TREE4	0.53	−0.73	1.11	0.77	0.91	56.30	45.30	−2.76
TREE5	1.31	−2.99	1.20	3.15	1.55	37.43	22.66	−2.12
TREE6	1.88	−2.28	2.34	3.67	0.58	28.04	19.96	−3.46
mean (SE)	1.62	−2.32	2.02	1.92	1.09	34.82	24.93	−2.67
	(0.25)	(0.35)	(0.29)	(0.49)	(0.17)	(4.57)	(4.14)	(0.23)

[a]Five parameters were calibrated: the proportionality parameters c_1 and c_2 defining C_S (Eqn 4), the proportionality parameters r_1 and r_2 defining R_X (Eqn 1) and the radial hydraulic resistance between the xylem and the storage compartment (R_S).
[b]C_S was estimated for two dates when Ψ_{PD} was measured (DOYs 208 and 234) and calculated on a storage volume basis.
[c]Ψ_{50} is the Ψ_{PD} causing 50% loss of maximum hydraulic conductance along the integrated root-to-leaf continuum.
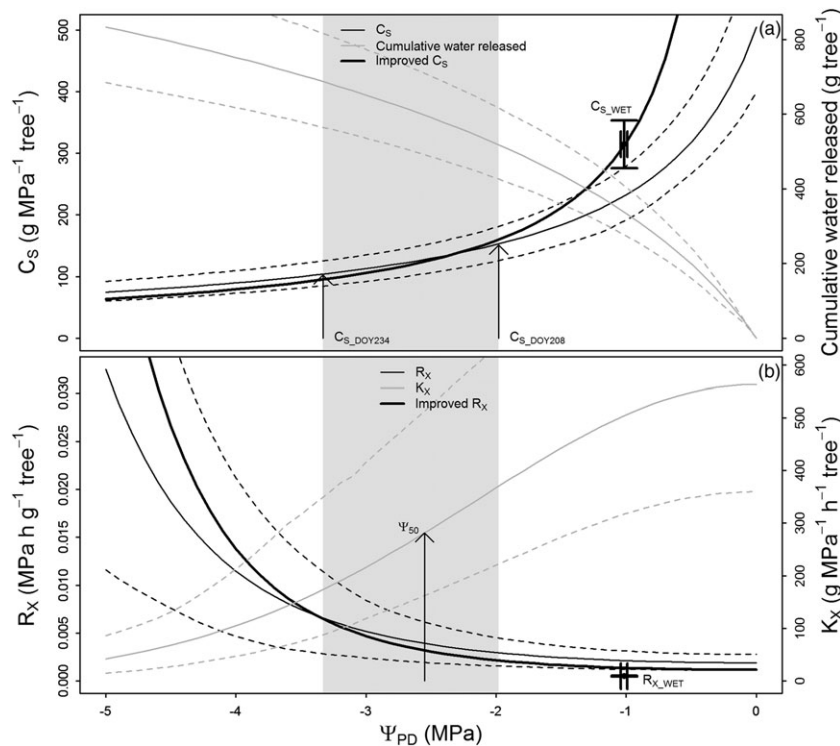
Figure 5. Hydraulic capacitance (C_S) and cumulative water released at the tree level (a), and hydraulic resistance (R_X) and conductance (K_X) in the root-to-leaf continuum (b) along a gradient of predawn water potential (Ψ_{PD}). Calibrated parameters obtained from six *Quercus ilex* trees during the dry period (Table 3) were used to estimate the mean (continuous line) and 95th and 5th percentile (dashed lines) curves of each variable. The calibrated parameters were obtained from a mechanistic model in which R_X (Eqn 1) and C_S (Eqn 4) were allowed to vary with Ψ_{PD}. Shaded areas indicate the modelled dry period, when average Ψ_{PD} ranged between −2.0 and −3.3 MPa. The curves of C_S and R_X adjusted for long-term (one-month) simulations of the dry period (in black) were improved by including values of the short-term (3–4 d) calibrations of the wet period (in red).

at the lower end of observations made in other species that may reach up to 19% when only elastic tissues are considered (see Table 3 in Betsch *et al*. 2011). The low reliance on stored water to maintain transpiration rates in *Q. ilex* might be related to the wood features of this species with relatively high wood density and small vessel size (Limousin *et al*. 2010a). These characteristics make trees more cavitation resistant to xylem tension, an adaptation which seems to be related to a limited capacity to reduce xylem tension via radial water release (Meinzer *et al*. 2008, 2009; Richards *et al*. 2014). This trade-off also explains that C_S of *Q. ilex* is at the lower end of reported values (see Fig. 5 in Meinzer *et al*. 2009 for comparison). Despite low $|f_S|$ / F_{STEM} ratios, the reliance on stored water increased with drought stress due to a more pronounced reduction in daily F_{STEM} compared to daily $|f_S|$. A similar pattern was also noticed in *Quercus robur* L., which used stored water primarily when subjected to drought stress (Matheny *et al*. 2015). These observations suggest greater relevance of stem water reservoirs to maintain transpiration rates and tree hydraulic integrity in future drier climates (see Tyree & Ewers 1991; and Bréda *et al*. 2006).

Model limitations

Two limitations related to the model structure and assumptions were detected during this study. Firstly, accurate simulations of diameter variations during the wet period were restricted to time frames of 3–4 d. Beyond this short time interval, diameter

simulations progressively deviated from measured values. During dry conditions, however, the length of the model period was not an issue because irreversible stem growth was prevented by soil water limitation (Lempereur *et al*. 2015). Any diameter variation during summer drought could be uniquely ascribed to radial water flow causing elastic stem shrinkage and swelling. In contrast, during the wet period when irreversible growth occurred, the carbon status of the plant is a factor involved in growth, for example via osmotic regulation of cell turgor and elongation (Lockhart 1965; Daudet *et al*. 2005). The lack of carbon-related equations in our water-based model describing sugar transport and/or carbon allocation to growth could explain inaccurate simulations when the modelled period extended beyond 3–4 d. Accordingly, the generally prescribed time frame for this model ranges from 1 d to 2 weeks (Steppe *et al*. 2006, 2008b). More sophisticated models integrating water and carbon transport processes should be further developed to simulate irreversible stem growth on a seasonal basis (De Schepper & Steppe 2010; Mencuccini *et al*. 2015; Steppe *et al*. 2015a).

Secondly, the model is theoretically designed to estimate C_S only for outer tissues, and we ignore the amount of water released by the xylem compartment. The contribution of the xylem to whole stem diameter variations is expected to be minor (Zweifel *et al*. 2000; Steppe & Lemeur 2004; Steppe *et al*. 2006), and our model therefore assumes the xylem as a rigid compartment and outer tissues – namely cambium, phloem and
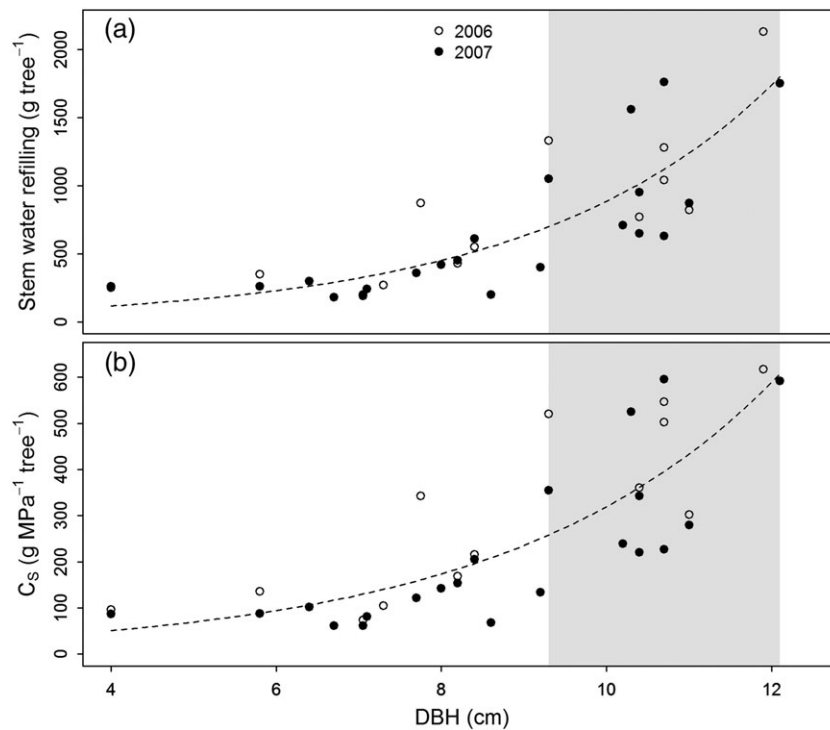
Figure 6. Stem water refilling (a) and hydraulic capacitance (C_S) (b) at the tree level estimated after the first heavy rain following the dry season. Two rain events registered in 2006 and 2007 (open and closed circles, respectively) met the minimum requirements to estimate stem storage capacity. Stem water refilling and C_S were estimated for a total of 23 *Quercus ilex* trees ranging in diameter at breast height (DBH) from 4 to 12.1 cm. Stem water refilling and C_S were exponentially related to tree DBH (Stem water refilling $= 30.27 \times \mathrm{e}^{(0.34 \times \mathrm{DBH})}$; $C_S = 15.05 \times \mathrm{e}^{(0.31 \times \mathrm{DBH})}$; $P < 0.001$). Shaded areas indicate the range in DBH of trees additionally surveyed for modelling.

phelloderm – as an elastic storage compartment responsible for diel shrinkage and swelling. Nevertheless, the amount of water released for a given change in volume is higher in the xylem than in the outer tissues, about 3.5 times higher in the case of savanna trees, which results in a greater capacitance of the xylem compartment (Scholz *et al.* 2007, 2008). Higher capacitance of the xylem can be ascribed to both elastic living parenchyma and the capacitive effect of cavitated conduits (Tyree & Ewers 1991; Hölttä *et al.* 2009; Richards *et al.* 2014). Thus, water release from the xylem could be important in large trees with a high proportion of sapwood and lumen volume (Waring *et al.* 1979; Hölttä *et al.* 2009; Betsch *et al.* 2011) or with large and numerous sapwood parenchyma rays such as *Q. ilex*. Models considering the capacitive effect of cavitation (Hölttä *et al.* 2009) and the xylem as an elastic compartment with a distinct elastic bulk modulus and hydraulic capacitance (Perämäki *et al.* 2005) would be necessary to further disentangle the contribution of elastic outer tissues and xylem parenchyma, and inelastic cavitated conduits to the overall capacitive discharge of water to the transpiration stream.

Simulated stem water release curves, root-to-leaf vulnerability curves and model validation

Simulations performed under dry conditions misestimated both C_S and R_X when extrapolated to a wider range of Ψ_{PD}

during wet conditions, and values obtained for well-watered conditions were also necessary to realistically describe the C_S and R_X curves over the entire Ψ_{PD} range (Fig. 5). This observation denotes that any extrapolation beyond the surveyed range of Ψ_{PD} must be taken with caution. More frequent measurements of Ψ_{LEAF} (or Ψ_X) would be necessary to re-calibrate model parameters at a higher temporal resolution (Steppe *et al.* 2008b) and obtain a more accurate evolution of C_S and R_X across a wider range of Ψ_{PD}.

Estimates of stem water refilling following first heavy rains at the end of the drought period and the vulnerability curves obtained by measurements at the organ scale were compared to model simulations. At the end of summer drought, the modelled cumulative water release averaged 683 g tree^{-1} at a Ψ_{PD} of -3.3 MPa (Fig. 5a), which is 60% of that estimated from the refilling calculations (1134 g tree^{-1} for a corresponding increase in Ψ_{PD} of 2.7 MPa, Fig. 6a). Likewise, mean C_S modelled across the range of surveyed conditions (from 103 to 314 g MPa^{-1} tree^{-1}, Fig. 5a) was lower than that estimated following heavy rains (414 g MPa^{-1} tree^{-1}, Fig. 6b). Inaccurate assumptions to estimate stem storage capacity and C_S using both approaches may account for this difference. Firstly, C_S could be overestimated from water refilling calculations because the corresponding water potential increase was measured several days apart from the refilling event and was therefore slightly underestimated. Besides, water refilling of branches and leaves incorrectly attributed to the stem may

overestimate the actual stem storage capacity. Secondly, C_S might be underestimated from model simulations due to the water release from xylem tissues (Scholz *et al.* 2008; Hölttä *et al.* 2009) undetected by our model. Models that integrate the hydraulic capacitance of the xylem compartment, continuous *in vivo* measurements of wood water content using frequency domain reflectometry (Matheny *et al.* 2015) or destructive sampling to obtain stem moisture release curves with psychrometers (Meinzer *et al.* 2003) might be complementary approaches to more accurately estimate the overall hydraulic capacitance of the stem. Likewise, direct measurements of Ψ_X would result in more accurate estimates of C_S than the simulated here, in which Ψ_X was inferred from Ψ_{LEAF} measurements.

On the other hand, variation in R_X as a function of drought stress affected to a lesser extent the model performance. The simulated vulnerability curve along the root-to-leaf continuum exhibited reasonable agreement with measurements made at the organ scale at the same site. The mean simulated Ψ_{50} was −2.67 MPa (Table 3). Estimates of Ψ_{50} in excised branches and roots of *Q. ilex* trees located at the same site averaged −3.88 and −2.39 MPa, respectively, using the air injection technique after flushing native embolism (Limousin *et al.* 2010a), and −4.7 MPa in branches using the bench drying technique (Martin-StPaul *et al.* 2014). Vulnerability to drought in the root-to-leaf continuum is determined to the greatest extent by the most vulnerable node along this hydraulic pathway (Baert *et al.* 2015). In this particular case, roots might be the major constrain to water flow along the root-to-leaf continuum, followed by stems and branches (Tyree & Ewers 1991; Sperry & Love 2015). Therefore, the integrated Ψ_{50} (−2.67 MPa) might primarily reflect the hydraulic vulnerability of roots. This alternative approach to generate integrated root-to-leaf vulnerability curves might be useful to describe the hydraulic functioning of the whole tree while avoiding to separately measure multiple hydraulic resistances (Baert *et al.* 2015), which might be controversial due to the strong variability in hydraulic conductance ascribed to methodological issues (Cochard & Delzon 2013; Martin-StPaul *et al.* 2014).

ACKNOWLEDGEMENTS

REFERENCES

Baert A., De Schepper V. & Steppe K. (2015) Variable hydraulic resistances and their impact on plant drought response modelling. *Tree Physiology* **35**, 439–449.

Barnard D.M., Meinzer F.C., Lachenbruch B., McCulloh K.A., Johnson D.M. & Woodruff D.R. (2011) Climate-related trends in sapwood biophysical properties in two conifers: avoidance of hydraulic dysfunction through coordinated adjustments in xylem efficiency, safety and capacitance. *Plant, Cell & Environment* **34**, 643–654.

Betsch P., Bonal D., Breda N., Montpied P., Peiffer M., Tuzet A. & Granier A. (2011) Drought effects on water relations in beech: the contribution of exchangeable water reservoirs. *Agricultural and Forest Meteorology* **151**, 531–543.

Bréda N., Huc R., Granier A. & Dreyer E. (2006) Temperate forest trees and stands under severe drought: a review of ecophysiological responses, adaptation processes and long-term consequences. *Annals of Forest Science* **63**, 625–644.

Brodersen C.R. & McElrone A.J. (2013) Maintenance of xylem network transport capacity: a review of embolism repair in vascular plants. *Frontiers in Plant Science* **4**, 108.

Campbell G.S. (1974) A simple method for determining unsaturated conductivity from moisture retention data. *Soil Science* **117**, 311–314.

Choat B., Jansen S., Brodribb T.J., et al. (2012) Global convergence in the vulnerability of forests to drought. *Nature* **491**, 752–755.

Cochard H. & Delzon S. (2013) Hydraulic failure and repair are not routine in trees. *Annals of Forest Science* **70**, 659–661.

Daudet F.-A., Améglio T., Cochard H., Archilla O. & Lacointe A. (2005) Experimental analysis of the role of water and carbon in tree stem diameter variations. *Journal of Experimental Botany* **56**, 135–144.

Epila J., De Baerdemaeker N.J.F., Vergeynst L.L., Maes W.H., Beeckman H. & Steppe K. (2017) Capacitive water release and internal leaf water relocation delay drought-induced cavitation in African Maesopsis eminii. *Tree Physiology* . DOI:10.1093/treephys/tpw128.

Goldstein G., Andrade J.L., Meinzer F.C., Holbrook N.M., Cavelier J., Jackson P. & Celis A. (1998) Stem water storage and diurnal patterns of water use in tropical forest canopy trees. *Plant, Cell & Environment* **21**, 397–406.

Granier A. (1985) Une nouvelle méthode pour la mesure du flux de sève brute dans le tronc des arbres. *Annals of Forest Science* **42**, 193–200.

Hölttä T., Cochard H., Nikimaa E. & Mencuccini M. (2009) Capacitive effect of cavitation in xylem conduits: results from a dynamic model. *Plant, Cell & Environment* **32**, 10–21.

Kocher P., Horna V. & Leuschner C. (2013) Stem water storage in five coexisting temperate broad-leaved tree species: significance, temporal dynamics and dependence on tree functional traits. *Tree Physiology* **33**, 817–832.

Lempereur M., Martin-StPaul N.K., Damesin C., Joffre R., Ourcival J.-M., Rocheteau A. & Rambal S. (2015) Growth duration is a better predictor of stem increment than carbon supply in a Mediterranean oak forest: implications for assessing forest productivity under climate change. *New Phytologist* **207**, 579–590.

Limousin J.M., Rambal S., Ourcival J.M., Rocheteau A., Joffre R. & Rodriguez-Cortina R. (2009) Long-term transpiration change with rainfall decline in a Mediterranean *Quercus ilex* forest. *Global Change Biology* **15**, 2163–2175.

Limousin J.M., Longepierre D., Huc R. & Rambal S. (2010a) Change in hydraulic traits of Mediterranean *Quercus ilex* subjected to long-term throughfall exclusion. *Tree Physiology* **30**, 1026–1036.

Limousin J.M., Misson L., Lavoir A.V., Martin N.K. & Rambal S. (2010b) Do photosynthetic limitations of evergreen *Quercus ilex* leaves change with long-term increased drought severity? *Plant, Cell & Environment* **33**, 863–875.

Lockhart J.A. (1965) An analysis of irreversible plant cell elongation. *Journal of Theoretical Biology* **8**, 264–275.

Martin-StPaul N.K., Longepierre D., Huc R., et al. (2014) How reliable are methods to assess xylem vulnerability to cavitation? The issue of "open vessel" artifact in oaks. *Tree Physiology* **34**, 894–905.

Matheny A.M., Bohrer G., Garrity S.R., Morin T.H., Howard C.J. & Vogel C.S. (2015) Observations of stem water storage in trees of opposing hydraulic strategies. *Ecosphere* **6**, 165.

McCulloh K.A., Johnson D.M., Meinzer F.C. & Woodruff D.R. (2014) The dynamic pipeline: hydraulic capacitance and xylem hydraulic safety in four tall conifer species. *Plant, Cell & Environment* **37**, 1171–1183.

Meinzer F.C., James S.A., Goldstein G. & Woodruff D. (2003) Whole-tree water transport scales with sapwood capacitance in tropical forest canopy trees. *Plant, Cell & Environment* **26**, 1147–1155.

Meinzer F.C., Woodruff D.R., Domec J.-C., Goldstein G., Campanello P.I., Gatti M.G. & Villalobos-Vega R. (2008) Coordination of leaf and stem water transport properties in tropical forest trees. *Oecologia* **156**, 31–41.

Meinzer F.C., Johnson D.M., Lachenbruch B., McCulloh K.A. & Woodruff D.R. (2009) Xylem hydraulic safety margins in woody plants: coordination of stomatal control of xylem tension with hydraulic capacitance. *Functional Ecology* **23**, 922–930.

Mencuccini M., Minunno F., Salmon Y., Martínez-Vilalta J. & Hölttä T. (2015) Coordination of physiological traits involved in drought-induced mortality of woody plants. *New Phytologist* **208**, 396–409.

Mouillot F., Rambal S. & Lavorel S. (2001) A generic process-based SImulator for meditERRanean landscApes (SIERRA): design and validation exercises. *Forest Ecology and Management* **147**, 75–97.

De Pauw D.J.W., Steppe K. & De Baets B. (2008) Identifiability analysis and improvement of a tree water flow and storage model. *Mathematical Biosciences* **211**, 314–332.

Perämäki M., Vesala T. & Nikinmaa E. (2005) Modeling the dynamics of pressure propagation and diameter variation in tree sapwood. *Tree Physiology* **25**, 1091–1099.

Rambal S., Ourcival J.-M., Joffre R., Mouillot F., Nouvellon Y., Reichstein M. & Rocheteau A. (2003) Drought controls over conductance and assimilation of a Mediterranean evergreen ecosystem: scaling from leaf to canopy. *Global Change Biology* **9**, 1813–1824.

Rambal S., Lempereur M., Limousin J.M., Martin-StPaul N.K., Ourcival J.M. & Rodríguez-Calcerrada J. (2014) How drought severity constrains gross primary production (GPP) and its partitioning among carbon pools in a *Quercus ilex* coppice? *Biogeosciences* **11**, 6855–6869.

Richards A.E., Wright I.J., Lenz T.I. & Zanne A.E. (2014) Sapwood capacitance is greater in evergreen sclerophyll species growing in high compared to low-rainfall environments. *Functional Ecology* **28**, 734–744.

Rodríguez-Calcerrada J., Li M., López R., et al. (2017) Drought-induced shoot dieback starts with massive root xylem embolism and variable depletion of nonstructural carbohydrates in seedlings of two tree species. *New Phytologist* **213**, 597–610.

Ruffault J., Martin-StPaul N.K., Rambal S. & Mouillot F. (2013) Differential regional responses in drought length, intensity and timing to recent climate changes in a Mediterranean forested ecosystem. *Climatic Change* **117**, 103–117.

Sack L., Cowan P.D., Jaikumar N. & Holbrook N.M. (2003) The "hydrology" of leaves: co-ordination of structure and function in temperate woody species. *Plant, Cell and Environment* **26**, 1343–1356.

De Schepper V. & Steppe K. (2010) Development and verification of a water and sugar transport model using measured stem diameter variations. *Journal of Experimental Botany* **61**, 2083–2099.

Scholz F.C., Bucci S.J., Goldstein G., Meinzer F.C., Franco A.C. & Miralles-Wilhelm F. (2007) Biophysical properties and functional significance of stem water storage tissues in Neotropical savanna trees. *Plant, Cell & Environment* **30**, 236–248.

Scholz F.C., Bucci S.J., Goldstein G., Meinzer F.C., Franco A.C. & Miralles-Wilhelm F. (2008) Temporal dynamics of stem expansion and contraction in savanna trees: withdrawal and recharge of stored water. *Tree Physiology* **28**, 469–480.

Sperry J.S. & Love D.M. (2015) What plant hydraulics can tell us about responses to climate-change droughts. *New Phytologist* **207**, 14–27.

Sperry J.S., Adler F.R., Campbell G.S. & Comstock J.P. (1998) Limitation of plant water use by rhizosphere and xylem conductance: results from a model. *Plant, Cell & Environment* **21**, 347–359.

Steppe K. & Lemeur R. (2004) An experimental system for analysis of the dynamic sap-flow characteristics in young trees: results of a beech tree. *Functional Plant Biology* **31**, 83–92.

Steppe K., De Pauw D.J.W., Lemeur R. & Vanrolleghem A. (2006) A mathematical model linking tree sap flow dynamics to daily stem diameter fluctuations and radial stem growth. *Tree Physiology* **26**, 257–273.

Steppe K., De Pauw D.J.W. & Lemeur R. (2008a) A step towards new irrigation scheduling strategies using plant-based measurements and mathematical modelling. *Irrigation Science* **26**, 505–517.

Steppe K., De Pauw D.J.W. & Lemeur R. (2008b) Validation of a dynamic stem diameter variation model and the resulting seasonal changes in calibrated parameter values. *Ecological Modelling* **218**, 247–259.

Steppe K., Cochard H., Lacointe A. & Améglio T. (2012) Could rapid diameter changes be facilitated by a variable hydraulic conductance? *Plant, Cell & Environment* **35**, 150–157.

Steppe K., Sterck F. & Deslauriers A. (2015a) Diel growth dynamics in tree stems: linking anatomy and ecophysiology. *Trends in Plant Science* **20**, 335–343.

Steppe K., Vandegehuchte M.W., Tognetti R. & Mencuccini M. (2015b) Sap flow as a key trait in the understanding of plant hydraulic functioning. *Tree Physiology* **35**, 341–345.

De Swaef T., De Schepper V., Vandegehuchte M.W. & Steppe K. (2015) Stem diameter variations as a versatile research tool in ecophysiology. *Tree Physiology* **35**, 1047–1061.

Tyree M. & Ewers F.W. (1991) The hydraulic architecture of trees and other woody plants. *New Phytologist* **119**, 345–360.

Verbeeck H., Steppe K., Nadezhdina N., et al. (2007) Atmospheric drivers of storage water use in Scots pine. *Biogeosciences* **4**, 657–671.

Waring R.H., Whitehead D. & Jarvis P.G. (1979) The contribution of stored water to transpiration in Scots pine. *Plant, Cell & Environment* **2**, 309–317.

Winsor C.P. (1932) The Gompertz curve as a growth curve. *Proceedings of the National Academy of Sciences* **18**, 1–8.

Zweifel R., Item H. & Häsler R. (2000) Stem radius changes and their relation to stored water in stems of young Norway spruce trees. *Trees – Structure and Function* **15**, 50–57.

Zweifel R., Steppe K. & Sterck F.J. (2007) Stomatal regulation by microclimate and tree water relations: interpreting ecophysiological field data with a hydraulic plant model. *Journal of Experimental Botany* **58**, 2113–2131.

SUPPORTING INFORMATION

Additional Supporting Information may be found in the online version of this article at the publisher's web-site:

Note S1. Mathematical equations and components of the water flow and storage model
Table S1. Value unit and definition of parameters used in the mechanistic water flow and storage model used to describe the hydraulic functioning of *Quercus ilex* trees
Figure S1. Ratio of the difference between predawn and midday stem water potential ($\Delta\Psi_X$ = midday Ψ_X − predawn Ψ_X) and the difference between predawn and midday leaf water potential ($\Delta\Psi_{LEAF}$ = midday Ψ_{LEAF} − predawn Ψ_{LEAF}) along a gradient of predawn water potential (Ψ_{PD}).